ADAPTIVE PATCH-BASED INPAINTING FOR IMAGE BLOCK RECOVERY

Yunqiang Liu

Barcelona Media - Innovation Center, University of Pompeu Fabra, Barcelona, Spain

Jin Wang, Huanhuan Zhang

Philips Research Asia - Shanghai, China

Keywords: Image block recovery, Inpainting, Error propagation, Combination strategy.

Abstract: This paper presents an adaptive patch-based inpainting algorithm for image block recovery in block-based coding image transmission. The proposed approach is based on prior information - patch similarity within the image. By taking advantage of the information, we recover the lost pixels by copying pixel values from the source based on a similarity criterion to keep local continuity. The pixel recovery is performed in a sequential fashion in which the recovered pixels can be used in the recovery process afterwards. In order to alleviate the error propagation with sequential recovery, we proposed an adaptive combination strategy which merges different directional recovered pixels according to the confidence of the estimated recovery performance. Experimental results show that the proposed method provides significant gains in both subjective and objective measurements.

1 INTRODUCTION

With the advent of multimedia communication, image/video transmission is becoming more and more important. Unfortunately, transmission error is inevitable on most channels such as wireless channels and the Internet which are not reliable enough to guarantee error-free transmission. Meanwhile, existing multimedia compression standards such as JPEG, MPEG-2 and H.264 (Sullivan and Wiegand, 2005) use the variable length coding (VLC) with block-based structure. The bit stream encoded by those standards is very sensitive to transmission errors (Kung et al., 2006). Even one single bit error may cause the loss of a whole block. And in video transmission, the mistakes in current blocks even propagate to the following blocks or the following frames, which will result in serious degradation in the visual quality of the decoded image.

Error recovery as a post-processing module is widely adopted to alleviate the negative effect of the erroneous blocks (Wang and Zhu, 1998) which attempts to reconstruct corrupted pixels utilizing the available neighbor information, without modifying source and channel coding schemes. Comparing to other existing error resilient approaches (Wang et al., 2000) as the Forward Error Correction and the interactive methods, no extra delay or redundant information will be added to the bit stream.

In general, according to correlation information, error recovery methods could be divided into two classifications (Agrafiotis et al., 2006): spatial error recovery (SER) and temporal error recovery (TER). The former utilizes spatial neighbor information to fill the missing area whereas the latter utilizes temporal information from successive frames. The spatial error recovery is often adopted in image sequence, intra coded frame and areas of low temporal redundancy in inter-coded frame.

A number of spatial recovery approaches have been proposed already in the literature. Bilinear interpolation (Wang et al., 2002) is a simple and efficient method which utilizes the nearest correctly decoded pixels to reconstruct the lost areas with weighted averages of these pixels. Rane et al. (Rane et al., 2002) estimate the lost information in the frequency domain based on the spatial smoothing constraint on the reconstructed blocks. While the obtained results are fairly good, these algorithms provide smooth reconstructions in image regions. Several methods try to

mitigate this problem by interpolating missing pixels along estimated edge directions such as directional interpolation (Kim et al., 2006) and verge points based method (Gao et al., 2007). In (Hong et al., 1999), error recovery is performed recursively for bands of missing pixels, using border pixels of surrounding blocks and already concealed pixels of the recovered block. The concept of sequential error recovery is also followed in the orientation adaptive sequential interpolation (OASI) approach (Li and Orchard, 2002).

Some methods address the problem of recovering missing data from different point of view. The best neighborhood matching (BNM) method (Wang et al., 1998) exploits block wise similarities within an image to replace whole missing blocks through a search process in the vicinity. Texture inpainting method, triggered in part by texture synthesis (Efros and Leung, 1999), has shown promising results on restoring corrupted image data, which is based on the similarity between their local neighborhood and the surrounding neighborhoods. Criminisi et al. (Criminisi and Perez, 2003) present an order-based image inpainting method that extends the texture synthesis approach by imposing higher priorities in the restoration order for pixels lying in the neighborhood of edges, thereby preserving better edge sharpness and continuity. In (Arias et al., 2009) the authors propose a non-local variational model to address the texture-oriented inpainting problem and provide impressive results. In (Bertalmio et al., 2003) Bertalmio et al. decompose the image into two functions, one for the texture ingredient and the other for the geometry structure of the image. Then they fill in the texture component using texture synthesis, and fill in the structure part using a classical inpainting approach based on partial differential equation models (Bertalmio et al., 2000) (Chan and Shen, 2001).

This paper presents an adaptive patch-based inpainting algorithm for image block recovery in block-based coding image transmission. The proposed approach is based on prior information - patch similarity within the image. By taking advantage of this information, we recover the lost pixels by copying pixel values from the source based on a similarity criterion to keep local continuity. The pixel recovery is performed in a sequential fashion in which the recovered pixels, as well as the uncorrupted pixels in the neighbor area, can be used in the recovery process afterwards. In order to alleviate the error propagation with sequential recovery, we proposed an adaptive combination strategy to reconstruct the lost block, which merges different directional recovered pixels according to their confidence. The confidence is estimated by the dissimilarity and the amount of reliable information in the patch.

The remainder of this paper is structured as follows. In Section 2, we give an overview of the proposed adaptive patch-based inpainting algorithm. Section 3 presents the proposed method in detail. Section 4 gives the results and comparisons, and conclusions are drawn in Section 5.

2 ALGORITHM OVERVIEW

Before the application of our image recovery approach, it is assumed that that we can locate the error region in the decoded video or image with some error detection algorithms. Most of traditional error recovery methods, such as bilinear interpolation, directional interpolation and OASI, perform as a low pass filter or directionally low pass filter in nature. They cannot recover accurately the sharp edge and texture within the lost region, however, the edge and texture information is very important for the human vision system. It is introduced by the following two reasons (Wang et al., 1998). First, the information source to estimate pixels in the missing blocks is the neighboring pixels in a very limited local region. Second, these methods rely on some predefined constraints on the lost blocks such as the recovered blocks should be smoothly connected with adjacent regions either in spatial or in transform domain.
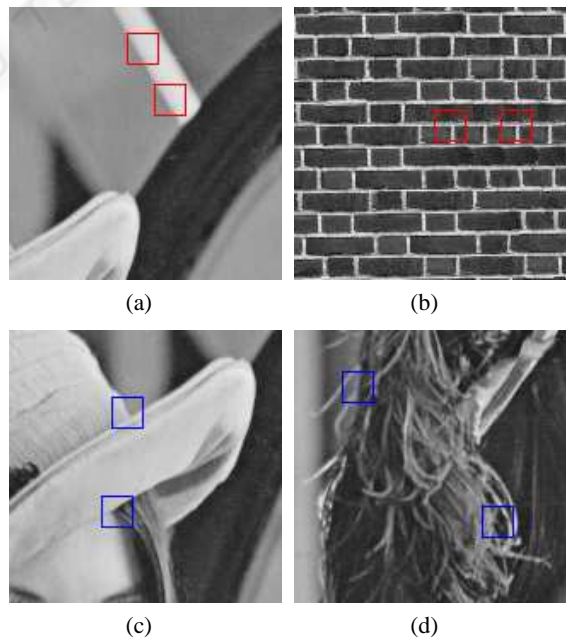
Figure 1: Textural and edge images.

In order to overcome the above problems, the BNM method exploits block wise similarities within an image to replace whole missing blocks through a search process in not only neighboring regions, but also remote regions within the image. The method can reconstruct the simple texture block (Figure 1(a)) and single strong edge (Figure 1(b)) effectively, and it can keep the sharp edge and details of texture in the lost block. However, BNM fails to recover the region with multiple edges (Figure 1(c)) or complex texture (Figure 1(d)), because there are much less matching possibilities for the lost blocks in the image. The BNM method takes the missing block as a whole to find a similar area in the vicinity. When the missing block is large, such as 8x8 or 16x16 which is very common in block-based image-coding systems, it is very difficult to find the similar area especially for the situation in Figures 1(c) and 1(d). Based on this observation, we adopt the approach of patch-based inpainting to reconstruct the missing regions. The approach grows the missing area pixel by pixel, based on prior information - patch-wise self-similarity within the image. By taking advantage of the information, we recover the lost pixels by copying pixel values from the source based on a similarity criterion to keep local continuity. The pixel recovery is performed in a sequential fashion in which the recovered pixels, as well as the uncorrupted pixels in the neighbor area, can be used in the recovery process afterwards (Li and Orchard, 2002). This sequential fashion introduces a bias on the later recovered pixels. Because the later recovered pixels depend on the previous recovered pixels, error propagation is inevitable. The quality of the recovered image is highly influenced by the order in which the filling process proceeds. The pattern of error propagation varies with the recovery order. In order to alleviate the error propagation with sequential recovery, we perform the patch-based inpainting algorithm from different directions. Then we calculate the confidence of the interpolated pixels from different directions, and finally combine them by adaptive weighting according to the confidence.

The proposed adaptive combination strategy is inspired by the work in (Li and Orchard, 2002). The authors adopt a linear merge strategy, in which the weights only depend on the distances of the given pixel to the four borders of the block. These distances cannot fully reflect the contribution of the pixels from different directions to the interpolated pixel. In our method, we introduced two confidence measurements to evaluate the contribution: reliability confidence and similarity confidence. The former measures the amount of the reliability of the available pixels for recovering the missing one. The latter evaluates the
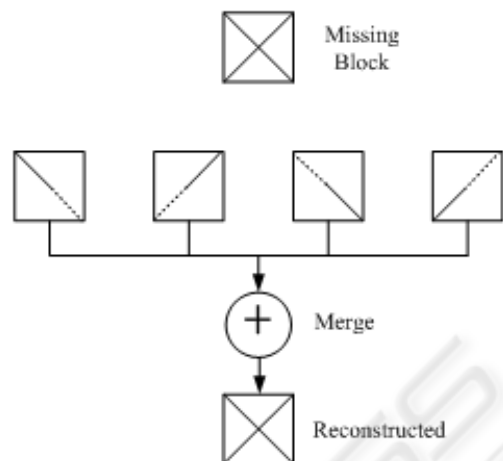
Figure 2: Reconstruction of lost blocks.

quality of the contribution of the available pixels to the interpolated pixel. And the final weights are determined by the two confidence measurements together. Based on the above analysis, the reconstruction of lost blocks follows three main steps:

a) Choose the scan direction as recovery order;

b) Patch-based inpainting for each determined direction;

c) Merge them by adaptive weighting according to the confidence.

3 ADAPTIVE PATCH-BASED INPAINTING

In the proposed adaptive patch-based inpainting algorithm, we first determine the recovery order for single-directional pixel interpolation. For each determined recovery order, we then recover the missing block using patch-based inpainting algorithm based on patch-wise similarity within the image. Finally, we reconstruct the missing block by an adaptive combination strategy according the confidence of the intermediate recovered pixels. A sketch map of the procedure of our method is shown in Figure 2.

3.1 Recovery Order

For single directional error recovery, error propagation is inevitable because the later recovered pixels depend on the previous recovered pixels. Different recovery orders may introduce different error propagation patterns. In practice, a specific recovery order is very effective for its specific area and direction of edge in the image. For example, the raster scanning order from left to right can reconstruct the horizontal

edge more accurately than the vertical edge. Moreover, the pixels in the top-left area can be recovered more accurately that those in the bottom-right area. Single order recovery cannot represent the correct and acceptable result especially for the area with complex structure. Each recovery order has its own advantage on its specific area and direction of edge in the image. Therefore, it is expected that we can reconstruct the image with high quality after carefully merging the result from different recovery order, as shown in Figure 2. Theoretically, if there are K continuous corrupted pixels, there are $K!$ different orders to get $K!$ recovery results(Li and Orchard, 2002). The computation is tremendous complex for searching all the orders. In fact, lots of recovery orders are not practical. For example the recovery beginning from the center of the corrupted areas has little available information. It is reasonable to choose several typical orders. In this way, the reconstructed quality doesn't decrease so much whereas the computation complexity decreases significantly. In our method, we use raster recovery order due to its simplicity of implementation. Starting from each corner, there are two directions to reach the diagonal corner and traversal all the missing pixels. Therefore, we adopt eight single-directional recovery orders, which is introduced by X. Li et al. the detailed information can be found in (Li and Orchard, 2002). Take the top-right corner as an example as shown in Figure 3, the recovery process starts from the pixels in the top-right corner, there are two directions to reach the diagonal corner. In Figure 3(a), it recovers the missing pixels with the direction from right to left for each line and repeats the process till the bottom-left corner. The missing block will be recovered using patch-based inpainting in each determined direction.

3.2 Patch-based Inpainting

For each determined recovery order, the patch-based inpainting algorithm uses patch-wise similarity within the image to reconstruct the missing block.

The missing block is referred to as the unknown area, denoted by Ω. The area will now be filled, pixel by pixel, in a raster fashion. The known area, denoted by Φ, provides samples used in the filling process. Let Ψ denote the patch. The patch may be a square, rectangle, triangle, or any other shape, and all the pixels within the patch are contiguously connected.

In this paper, the patch centered at the pixel $p_0 = (i, j)$ is here defined to be a diamond shaped window, as:

$$\Psi(p_0) = \{p = (x, y), 0 \leq (|x-i| + |y-j|) \leq T_0\} \quad (1)$$

where T_0 is the order of the patch, which controls

the size of the patch. A target patch with $T_0 = 2$ is shown in Figure 4, where the light-gray pixel p is the current pixel to be recovered, and the dark-gray pixels represent the available pixels, available means uncorrupted or recovered, the white pixels are the missing pixels. A source patch is the corresponding area in Φ, which has the same shape and size as the target patch.

(a)   (b)
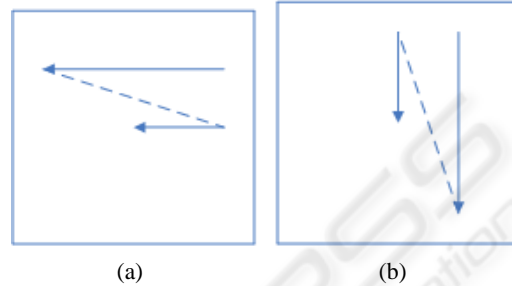
Figure 3: Textural and edge images.

To recover the lost pixels, a search procedure is applied within a large range in the image. The purpose of the search procedure is to find a source patch in the image that has the best similarity with the target patch. We then replace the current pixel being filled in the lost block by the value of the corresponding pixel of the best matched source patch, as shown in Figure 5. Then we recover the rest of pixels using the same approach under the mentioned recovery order.
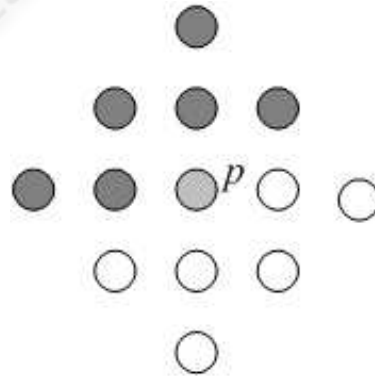
Figure 4: Target patch with the order of 2.

The similarity of the source patch and the target patch is measured by the normalized sum of absolute differences. Since it is desirable to give more importance to the pixels that are uncorrupted than those recovered previously, different weights are taken for the two kinds of pixels. The pixels within the patch that have not been recovered yet are not taken into account in the distance. The distance between the source patch and target patch can thus be expressed as:
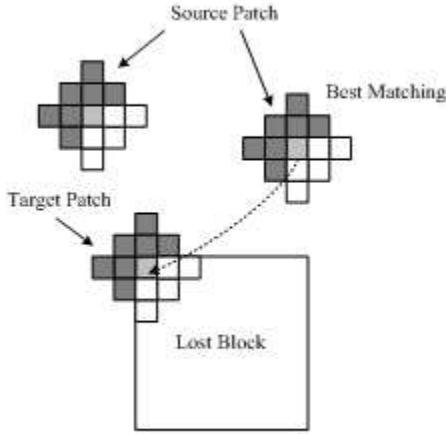
Figure 5: Pixel recovery.

$$d(\Psi(p_s), \Psi(p_t)) = \frac{\sum\limits_{q \in \Psi(q_0)} a(p_t + q)|f(p_s + q) - f(p_t + q)|}{\sum\limits_{q \in \Psi(q_0)} a(p_t + q)}$$

(2)

where p_s and p_t are the centers of the source patch $\Psi(p_s)$ and the target patch $\Psi(p_t)$, respectively, $f(p)$ is the value of the pixel p, $\Psi(q_0)$ is the diamond window defined in (1) and $q_0 = (0,0)$, The weight map $a(p)$ is assigned for each pixel in target patch, as follows:

$$a(p) = \begin{cases} 1, & p \text{ is uncorrupted} \\ 0.5, & p \text{ is revcovered} \\ 0, & p \text{ is lost} \end{cases}$$

(3)

The recovered pixel has some distortion and is given a lower weight compared with the uncorrupted one. And $a(p)$ is set to 0.5 for the recovered pixel, experimentally.

In summary, the patch based inpainting algorithm for single directional recovery proceeds as follows:

1. Choose a pixel to be recovered in Ω as current pixel according to the predetermined recovery order, such as that in Figure 3(a).

2. Get the target patch $\Psi(p_t)$ centered by the current pixel, and search as the best matching source patch $\Psi(p_s)$ with $\Psi(p_t)$, which minimizes $d(\Psi(p_s), \Psi(p_t))$. In this paper, the search range is selected as 32×32.

3. Copy the pixel in the center of the source patch to the current pixel. Alternatively, in order to accelerate the computation, we can fill all the unknown pixels in the target patch by the corresponding pixels in the source patch. In this case, the computation will be decreased significantly with acceptable reduction of the performance.

4. Repeat steps 1, 2, and 3 until all the lost pixels are filled.

3.3 Combination Strategy

In single-directional inpainting, the error of restored pixels will increase along the recovery direction because of unconfident recovered pixel results. Different recovery orders may introduce different error propagation patterns. The error from one recovery order can be compensated by results from the other order. Therefore, we can reconstruct the image through merging the result from different recovery orders as:

$$p = \sum_{n=1}^{8} w_n(p) f(p_n)$$

(4)

where $w_n(p)$ is the weighting coefficient controlling the contribution of the nth recovery order for the pixel p, and $f(p_n)$ is the value of the recovered pixel in the nth order.

In this paper, the weight is associated with the confidence of the recovery performance in a specific recovery order. The confidence consists two items: similarity confidence $S_n(p)$ and reliablility confidence $R_n(p)$.

The similarity confidence $S_n(p)$ can be expressed by the Gaussian function of the Euclidean distance between the source patch and the target patch, and we simplified it as:

$$S_n(p) = 2^{-\alpha d^*(\Psi(p_s), \Psi(p_t))}$$

(5)

where $d^*(\Psi(p_s), \Psi(p_t))$ is the difference between the target patch and the best match source patch, which is defined in (2), and the parameter α regulates the relative influence of the difference on the weights. It is set to 0.125, experimentally.

The reliability confidence $R_n(p)$ measures the amount of reliable information surrounding the pixel p. Our aim is to give higher weight to the pixel whose patch has more pixels which are known or have already been recovered. $R_n(p)$ is defined as:

$$R_n(p) = \frac{\sum\limits_{q \in \Psi(p)} R_n(q)}{A(\Psi(p))}$$

(6)

where $\Psi(p)$ is the target patch centered on the pixel p, $A(\Psi(p))$ is the area of the patch $\Psi(p)$, i.e. the number of pixels in the patch. Initially, we define $R_n(p) = 0$ if p is a missing pixel, $R_n(p) = 1$ if not.

For each pixel p to be recovered, we define its weight for a specific recovery order associated with the product of above two terms:

$$w_n(p) \propto S_n(p) R_n(p)$$

(7)

The weighting provides an efficient and flexible way to select the appropriate pixels contributing to the estimation of the lost pixel for the final result.

We compute the confidence for all the recovery order for each lost pixel, and normalize the weight coefficients as:

$$w_n(p) = \frac{S_n(p)R_n(p)}{\sum\limits_{k=1}^{8} S_k(p)R_k(p)} \tag{8}$$

After obtaining these weight coefficients, we recover the lost pixels through combining the intermediate results from all the recovery orders.

4 EXPERIMENT RESULTS

In order to illustrate the performance of our error recovery method, we take many experiments on test images: Lena, Baboon, Pepper and Barbara. We consider the situation of the 16×16 block since the image or video are often encoded in 16×16 block size. Different block-loss situations are investigated in the paper: isolated block loss and consecutive block loss. For objective evaluation, we use a modified peak signal-to-noise ratio (PSNR) as the objective measure in our experiments, which is defined just on the corrupted areas instead of the entire image:

$$PSNR = 10\log_{10} \frac{255}{\frac{1}{M} \sum\limits_{p \in \Omega} (f_0(p) - f_r(p))} \tag{9}$$

where $f_o(p)$ and $f_r(p)$ are the pixel values in the original and the recovered image, and M is the number of the lost pixels. We first give the implementation details in our experiments and then compare it with several existing error recovery algorithms.

4.1 Implementation Details

For the implementation of the proposed algorithm, there remain some choices, which include the following:

1. **The patch size.** The size of the patch affects how well the filled pixels capture the local characteristics of the known region. The patch size is controlled by T_0, which is defined in (1).

2. **The filling manner.** The filling manner means whether the pixel centered on the target patch (pixel-filling) or the unknown part of the target patch (patch-filling) will be filled in the step 3 of the patch based inpainting algorithm.

In the first experiment, we illustrate how the choice of patch size affects the recovery performance. We fix the search range as 32×32 with pixel-filling. And we investigate the isolated block loss situation with about 10% loss rate. Table 1 shows the evolution of PSNR values with different patch size using pixel-filling. Smaller patch size allows more matching possibilities, thus implies weaker statistical constraints. Up to a certain limit, bigger patch size can capture the texture characteristics better, however with much higher computation complexity. From the results in Table 1, $T_0 = 2$ is a good balance.

Table 1: The impact of patch size for block loss (dB).

T_0	Lena	Baboon	Pepper	Barbara
1	26.63	20.94	28.34	24.13
2	27.35	21.25	29.10	26.01
3	27.33	21.24	29.31	26.40

Table 2: The impact of patch size for block loss (dB).

Filling	Lena	Baboon	Pepper	Barbara
Pixel	27.35	21.25	29.10	26.01
Patch	27.06	20.88	28.12	25.94

Table 3: Performance comparison for isolated block loss (dB).

Image	BI	OI	OASI	Ours
Lena	24.03	23.74	25.98	27.35
Baboon	20.25	18.46	20.16	21.25
Pepper	24.85	24.34	26.67	29.10
Barbara	20.69	21.62	22.84	26.01

In the second experiment, we demonstrate the impact of the filling manner on the recovery performance. Table 2 shows the performance of the two different filling manners with $T_0 = 2$. It can be seen that pixel-filling shows better performance than the patch-filling and the gap ranges from 0.07 to 0.98 dB.

4.2 Comparison Results

To demonstrate the effectiveness of our algorithm, we compare it with several previous existing error recovery algorithms: bilinear interpolation (BI), the orientation adaptive sequential interpolation (OASI) (Li and Orchard, 2002), order-based inpainting (OI) (Criminisi and Perez, 2003). For our algorithm, in the experiment, we set $T_0 = 2$ and use pixel-filling manner in the recovery process.

Table 3 and Table 4 give the PSNR comparisons between the compared methods and our algorithm under the following two loss situations: the isolated block loss (about 10%) and consecutive block loss

Table 4: Performance comparison for consecutive block loss (dB).

Image	BI	OI	OASI	Ours
Lena	22.21	21.32	22.07	24.21
Baboon	19.15	17.94	19.08	20.24
Pepper	25.22	23.26	24.00	26.05
Barbara	19.98	18.21	20.06	23.11

(a) Origin (b) Corrupted

(c) Bilinear Interpolation (d) Order-based Inpainting

(e) OASI (f) Our Method
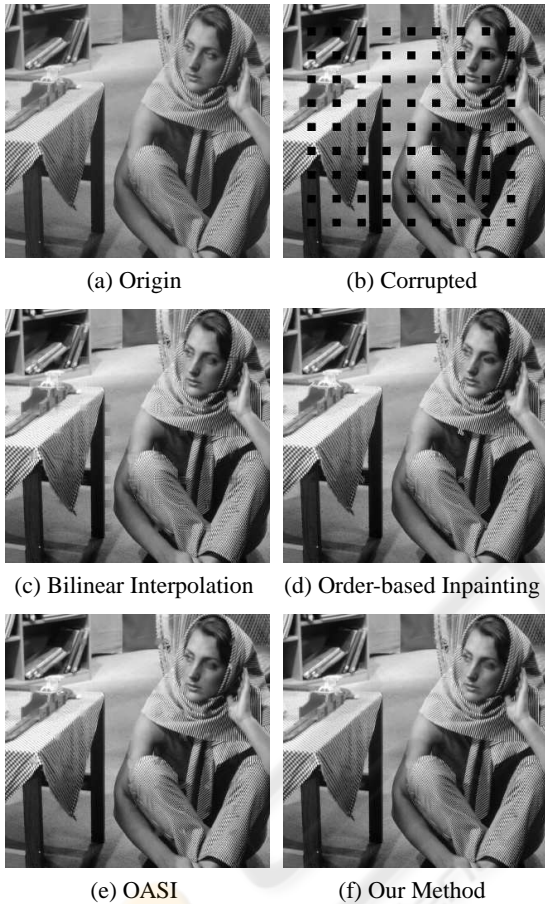
Figure 6: Reconstructed images for Barbara for isolate block loss.

(about 25%). It can be seen that we have achieved 1.09-3.17 dB improvement in the case of isolated block loss and 1.16-3.05 dB improvement in the case of consecutive block loss over OASI. To subjectively evaluate the results, Figure 6 shows the comparison of the reconstructed images for Barbara by the compared methods and our algorithm in the situation of isolated block loss. It can be observed that our new approach has achieved significant improvements in the area of complex texture structures. For better subjective evaluation, we show some enlarged examples for sharp edge areas, texture areas and very complex areas in Figure 7. The visual quality of the recov-

(a) Bilinear Interpolation (b) Order-based Inpainting

(c) OASI (d) Our Method
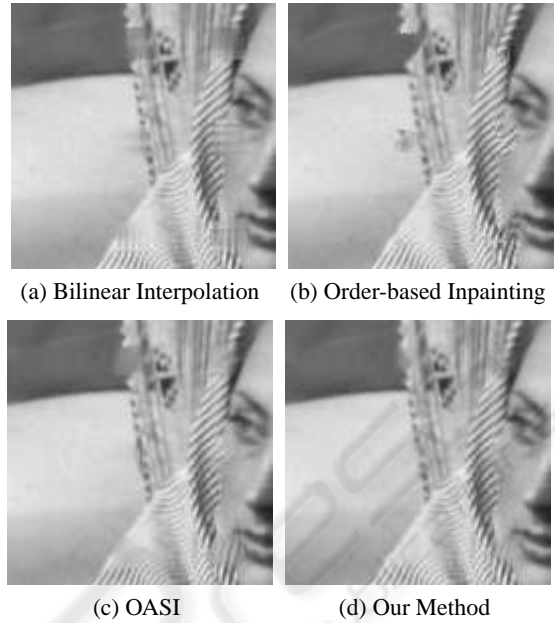
Figure 7: Enlarged part of the images in Figure 6.

ered blocks are very good even when the areas contain a lot of detail information. Figure 8 shows the comparison of the reconstructed images for Lena by the compared methods and our technique in the situation of consecutive block loss. Significant improvements can be found in the recovered image by the proposed method, especially on the blocks with the strong edges or complex texture. And the similar results are obtained for other test images.

5 CONCLUSIONS

In this paper, we present an adaptive patch-based inpainting algorithm for image block recovery in block-based coding image transmission. The proposed approach is based on a prior information - patch similarity within the image. By taking advantage of the information, we recover the lost pixels by copying pixel values from the source based on a similarity criterion to keep local continuity. The pixel recovery is performed in a sequential fashion in which the recovered pixels can be used in the recovery process afterwards. In order to alleviate the error propagation with sequential recovery, we proposed an adaptive combination strategy which merges different directional recovered pixels according to the confidence of the estimated recovery performance. Experimental results show that the proposed method provides significant improvements in terms of both subjective and objective evaluations.

(a) Origin   (b) Corrupted

(c) Bilinear Interpolation   (d) Order-based Inpainting

(e) OASI   (f) Our Method
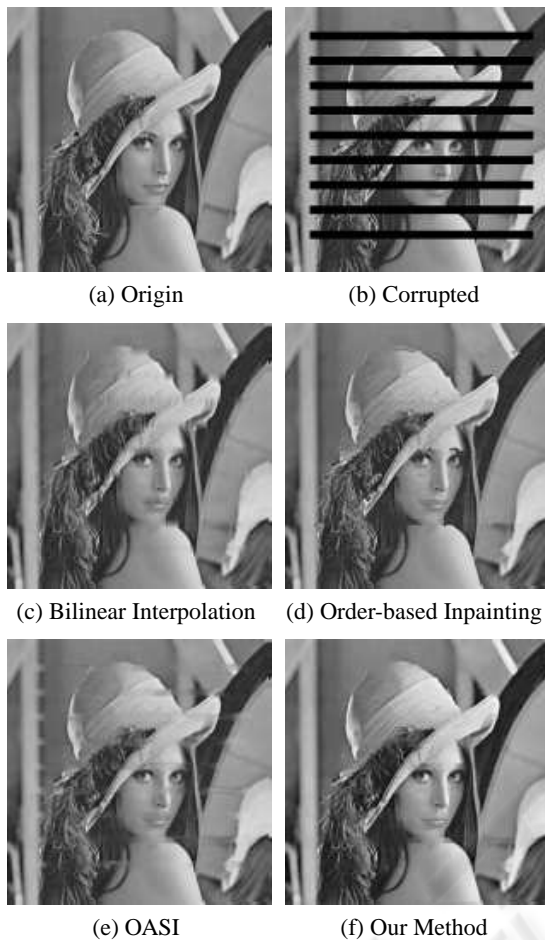
Figure 8: Reconstructed images for Lena for consecutive block loss.

ACKNOWLEDGEMENTS

REFERENCES

Agrafiotis, D., Bull, D., and Canagarajah, C. (2006). Error resilient video coding techniques. *IEEE Trans. Circuits Syst. Video Technol.*, 16(8):960–973.

Arias, P., Caselles, V., and Sapiro, G. (2009). Variational framework for non-local image inpainting. In *Proc.EMMCVPR*, pages 345–358, Bonn, Germany.

Bertalmio, M., Sapiro, G., Caselles, V., and Ballester, C. (2000). Image inpainting. In *Proc. Computer Graphics (SIGGRAPH 2000)*, pages 417–424.

Bertalmio, M., Vese, L., Sapiro, G., and Osher, S. (2003). Simultaneous structure and texture image inpainting. *IEEE Trans. on Image Processing*, 12(8):882–889.

Chan, T. and Shen, J. (2001). Mathematical models for local nontexture inpainting. *SIAM J. Appl. Math.*, 62(3):1019–1043.

Criminisi, A. and Perez, P. (2003). Object removal by exemplar-based inpainting. In *Proc. Int. Conf. Comp. Vision Pattern Rec.*, pages 721–728, Madison, WI.

Efros, A. and Leung, T. (1999). Texture synthesis by non-parametric sampling. In *Proc. Int. Conf. Computer Vision*, pages 1033–1038, Kerkyra, Greece.

Gao, Y., Wang, J., Liu, Y., Yang, X., and Wang, J. (2007). Spatial error concealment technique using verge points. In *Proc. IEEE ICASSP*, pages 309–312, Honolulu, HI.

Hong, M. C., Scwab, H., Kondi, L., and Katsaggelos, A. K. (1999). Error concealment algorithms for compressed video. *Signal Processing: Image Communication*, 14:473–492.

Kim, W., Koo, J., and Jeong, J. (2006). Fine directional interpolation for spatial error concealment. *IEEE Trans. Consumer Electronics*, 52(3):1050–1055.

Kung, W.-Y., Kim, C.-S., and Kuo, C.-C. J. (2006). Spatial and temporal error concealment techniques for video transmission over noisy channels. *IEEE Trans. Circuits Syst. Video Technol.*, 16:789–802.

Li, X. and Orchard, M. T. (2002). Novel sequential error-recovery techniques utilizing orientation adaptive interpolation. *IEEE Trans. Circuits Syst. Video Technol.*, 12(10):857–864.

Rane, S. D., Remus, J., and Sapiro, G. (2002). Wavelet-domain reconstruction of lost blocks in wireless image transmission and packet-switched networks. In *Proc.IEEE ICIP*, pages 309–312, Rochester, NY.

Sullivan, G. J. and Wiegand, T. (2005). Video compression - from concepts to the H.264/AVC standard. *Proceedings of the IEEE*, 93(1):18–31.

Wang, Y., Hannuksela, M. M., Varsa, V., Hourunranta, A., and Gabbouj, M. (2002). The error concealment feature in the H.26L test model. In *Proc. IEEE ICIP*, pages 729–732, Rochester, NY.

Wang, Y., Wenger, S., , and Katsaggelos, A. K. (2000). Error resilient video coding techniques. *IEEE Signal Processing Mag.*, 17(4):61–82.

Wang, Y. and Zhu, Q.-F. (1998). Error control and concealment for video communication: A review. *Proceedings of the IEEE*, 86(5):974–997.

Wang, Z., Yu, Y., and Zhang, D. (1998). Best neighborhood matching: An information loss restoration technique for block-based image coding systems. *IEEE Trans. on Image Processing*, 7(7):1056–1061.